2003

A Novel Electrodeposition Process for Plating Zn-Ni-Cd Alloys

Hansung Kim
University of South Carolina - Columbia

Branko N. Popov
University of South Carolina - Columbia, popov@engr.sc.edu

Ken S. Chen

Publication Info

Journal of the Electrochemical Society, 2003, pages C81-C88.

Journal of The Electrochemical Society, **150** (2) C81-C88 (2003)
0013-4651/2003/150(2)/C81/8/$7.00 © The Electrochemical Society, Inc.

A Novel Electrodeposition Process for Plating Zn-Ni-Cd Alloys

Hansung Kim,[a,*] Branko N. Popov,[a,,z] and Ken S. Chen[b,**]**

[a]*Center for Electrochemical Engineering, Department of Chemical Engineering, University of South Carolina, Columbia, South Carolina 29208, USA*
[b]*Sandia National Laboratories, Engineering Sciences Center, Albuquerque, New Mexico 87185-0834, USA*

Zn-Ni-Cd alloy was electrodeposited from an alkaline electrolytic bath under potentiostatic conditions. Bath analyses using a pH concentration diagram reveal that addition of a complexing agent is essential to maintain the bath stability. Introduction of a low concentration of $CdSO_4$ reduces the anomalous nature of the Zn-Ni deposit. Deposits obtained from the electrolytic bath which contains 60 g/L of $ZnSO_4 \cdot 7H_2O$, 40 g/L of $NiSO_4 \cdot 6H_2O$, 1 g/L of $CdSO_4$, and 80 g/L of $(NH_4)_2SO_4$ in the presence of additives and ammonium hydroxide at pH 9.3 has a composition of 50 wt % of Zn, 28 wt % of Ni, and 22 wt % of Cd. By optimizing the Cd concentration in the bath, it is possible to control the amount of Ni in the deposit. At large overpotentials, the surface of the electrode is covered with hydrogen which lowers the deposition current density. Rotating disk electrode studies indicated that the deposition of Cd is under mass control, while Ni deposition is under kinetic control.
 [DOI: 10.1149/1.1534599]

Manuscript received March 25, 2002. Available electronically January 6, 2003.

Zinc, by the virtue of its low standard electrode potential [$E^o = -0.76$ V *vs.* normal hydrogen electrode (NHE)] is a very active metal, which corrodes easily. This characteristic of zinc makes it more suitable to act as a sacrificial coating on many metals and alloys with standard electrode potentials higher than that of zinc. The difference in electronegativity of the coating and the substrate serves as the driving force for the corrosion of the sacrificial coating under corroding conditions. Owing to the very large difference in electronegativity of Zn and Fe, rapid dissolution of Zn happens under corroding conditions. The problem of accelerated corrosion of Zn can be overcome by alloying it with another metal, which will bring the standard electrode potential of the alloy much closer to that of the substrate metal while still remaining on the cathodic side to provide sacrificial protection.

Ni, Co, Fe are some of the alloying metals that have been used to decrease the corrosion potential of the coating.[1-6] Zn-Ni alloys possess better corrosion resistance compared to zinc and have been studied extensively for automotive applications. The codeposition of Zn-Ni is anomalous and a higher percent of Zn is present in the final deposit. The mechanism for this preferential deposition has been discussed extensively in the literature.[7-9] Typical nickel composition in the alloy is approximately 10%, and any further increase in nickel composition is based on using a higher than predicted Ni/Zn ratio in the bath.[10,11] An enhancement in the nickel composition would lead to more anodic open-circuit potential, which in turn will reduce the driving force for the galvanic corrosion. Also the barrier properties associated with nickel-rich deposits are superior compared to other coatings.

Inclusion of ternary elements like P, Sn, SiO_2, Al_2O_3, has been found to improve the corrosion resistance of the Zn-Ni alloy by enhancing the amount of Ni in the codeposit.[12-15] These elements are also known to improve electrical, mechanical, magnetic properties, and corrosion resistance properties of the alloy.

We recently developed an acid-based electrodeposition process to deposit Zn-Ni-Cd ternary alloy composites, with varying proportions of cadmium (6-30 wt %) in the coating. Preliminary studies based on corrosion and brittleness characteristics indicate that this alloy can serve as a potential candidate for replacing Cd and Zn-Ni deposition due to its better corrosion resistance and permeation resistance properties.[16,17] A very small amount of $CdSO_4$ (1-3 g/L) was used along with the Zn-Ni bath to deposit the ternary alloy. However, it was observed that the deposit from the acid bath showed poor adherence, and the deposit properties deteriorated with increase in concentration of $CdSO_4$ in the bath.[18]

The objective of this study was to develop a superior Zn-Ni-Cd alloy with good adherence and stability for a wide range of Cd content in the bath. This has been accomplished by using an alkaline bath. Stripping cyclic voltammogram and surface morphology characterization techniques have been used extensively to understand the Zn-Ni-Cd deposition process.

Experimental

Zn-Ni-Cd alloy deposition was carried out on mild steel foils of thickness 0.5 mm and area 50 × 50 mm from an alkaline bath containing different amounts of $NiSO_4 \cdot 6H_2O$, $ZnSO_4 \cdot 7H_2O$, and $CdSO_4$ in the presence of $(NH_4)_2SO_4$. The amount of ammonium sulfate was fixed at 80 g/L. Ammonium hydroxide was also added to act as a complexing agent to prevent the precipitation of metal ion as hydroxide forms. The steel substrates were subjected to a pretreatment involving mechanical polishing with alumina powder and various grades of polishing paper followed by degreasing with soap solution. Depositions were carried out in a three-electrode setup using an EG&G PAR (type 273A) potentiostat/galvanostat. A standard calomel electrode (SCE) was used as the reference electrode and a platinum mesh served as the counter electrode. All the depositions were carried out potentiostatically at room temperature. The morphology of the alloys deposited under various conditions was studied using scanning electron microscopy (SEM). Composition analysis was carried out by averaging the energy dispersive X-ray (EDX) data obtained from ten different sites.

Results and Discussion

Stripping cyclic voltammogram (SCV).—SCV was used to obtain preliminary information about the Zn-Ni-Cd deposition process. Electrodeposition of Zn-Ni-Cd was carried out on a platinum rotating disk electrode from a solution containing 1 g/L of $CdSO_4$, 20 g/L of $NiSO_4 \cdot 6H_2O$, 40 g/L of $ZnSO_4 \cdot 7H_2O$, and 0.5 M Na_2SO_4. Figure 1 shows the SCV analysis of Zn-Ni-Cd depositions obtained at different rotation speeds. The potential scan of the SCV began at 0 V *vs.* SCE in the cathodic direction until −1.5 V *vs.* SCE after which the scan was reversed to come back to the starting point. During the cathodic scan, the deposition of Zn, Ni, and Cd proceeds along with the hydrogen evolution reaction. The deposition currents begin to increase after about −0.9 V and rises indefinitely due to accompanying hydrogen evolution reaction. During the anodic scan distinct peaks were observed which could be attributed to the dissolution of alloy components. Based on the potentials at which these peaks occur, one can make a qualitative estimate of the alloy composition. The first peak that is seen at around −0.8 V *vs.* SCE

* Electrochemical Society Student Member.
** Electrochemical Society Active Member.
z E-mail: popov@engr.sc.edu

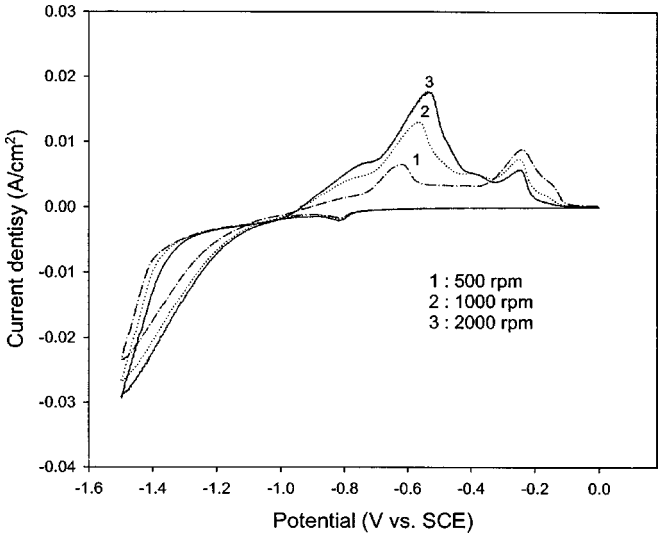

Figure 1. Linear sweep voltammetry of Zn-Ni-Cd film electrodeposited from electrolyte containing 1 g/L of $CdSO_4$, 20 g/L of $NiSO_4 \cdot 6H_2O$, 40 g/L of $ZnSO_4 \cdot 7H_2O$, and 0.5 M Na_2SO_4. Scan rate = 30 mV/s at different rotating speeds.

corresponds to the Zn dissolution.[19] Based on the potential at which the peak occurs (−0.6 V *vs.* SCE), the second anodic dissolution peak can be thought to be due to the dissolution of Cd-rich phase. The third dissolution peak that is seen in the anodic scan of the SCV is attributed to the dissolution of Ni-rich phase. When the rotation speed is increased, the Cd and Zn dissolution peaks increase indicating the mass-transfer controlled nature of the deposition processes, which are in agreement with previous studies.[19] The Ni-dissolution peak, on the contrary, decreases with increasing the rotation speed. Nickel deposition is kinetic controlled,[20] and the observed decrease in nickel content in the codeposit is merely due to the effect of accompanying side reactions that are under mass-transfer control. With this knowledge about the deposition process, we next proceed to study the effect of bath composition on the deposit composition.

Effect of Cd concentration.—Figure 2 shows the effect of $CdSO_4$ concentration and deposition potential on the composition of Zn-Ni-Cd ternary alloy. The concentration of $CdSO_4$ was varied from 0.5 to 3 g/L while the concentration of $ZnSO_4 \cdot 7H_2O$ and $NiSO_4 \cdot 6H_2O$ were fixed as 10 and 40 g/L, respectively. The bath pH was maintained at 9.3, and the depositions were done without any stirring of solution.

As was shown in the stripping cyclic voltammetry studies, cadmium and zinc depositions are mass-transfer controlled while nickel deposition is kinetically controlled. For this reason, the applied potential of electrodeposition and concentrations of the electroactive species largely affect the deposit composition and thereby the properties. When electrodeposition is carried out at potentials of −1.0 V *vs.* SCE, the concentration of Cd dominates in the deposit because of its low reduction potential when compared to that of Zn. Ni also has a low equilibrium potential, but it has a high activation overpotential for the deposition to occur at room temperature. In the case of acid sulfate bath at pH 2.5, Ni deposition occurs at −0.9 V *vs.* SCE, which is a much more cathodic potential than its standard potential.[19] Further increase in the deposition potential results in an increase in the concentrations of Zn and Ni in the deposit. When

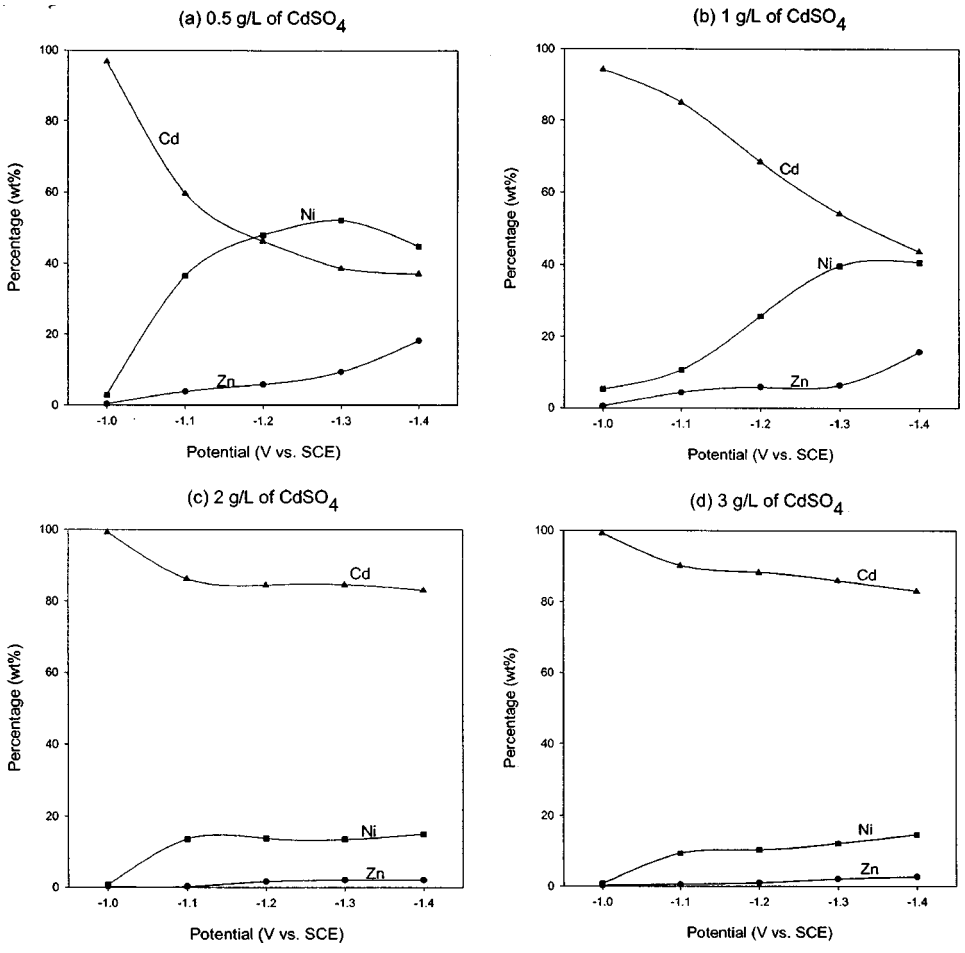

Figure 2. Effect of $CdSO_4$ concentration on the alloy composition as a function of the applied potential. $ZnSO_4 \cdot 7H_2O$, 10 g/L; $NiSO_4 \cdot 6H_2O$, 40 g/L; pH 9.3, without stirring.

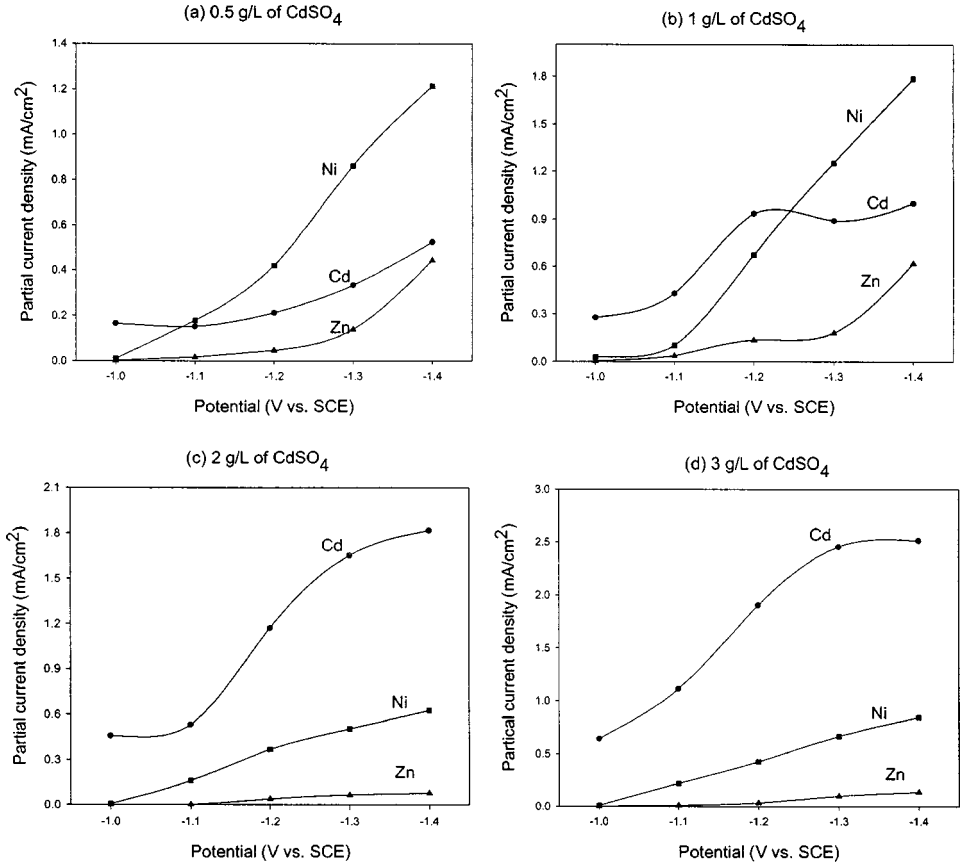

Figure 3. Effect of $CdSO_4$ concentration on the partial current density as a function of the applied potential. $ZnSO_4 \cdot 7H_2O$, 10 g/L; $NiSO_4 \cdot 6H_2O$, 40 g/L; pH 9.3, without stirring.

$CdSO_4$ concentration in the bath is increased beyond 2 g/L, deposition of Zn is completely suppressed, and there is a complete domination of Cd in the deposit. For a better understanding of the deposition process, the partial current densities of each component were calculated using Faraday's law. Figure 3 shows a plot of the partial current densities of Zn, Cd, and Ni as a function of electrodeposition potential. When the concentration $CdSO_4$ in the bath is $\leqslant 1$ g/L, increasing the applied potential has an effect on the composition of the deposits because the limiting current of Cd is lower than the partial current density of Ni. Since Cd deposition is mass-transfer controlled, the concentration of Cd in the deposit does not increase once the limiting current density for deposition is reached. However, a further increase in the concentration of $CdSO_4$ leads to an increase in the limiting current density thereby resulting in a complete domination of Cd deposition. The deposits contain about 80 wt % of Cd (Fig. 2) under these conditions, and increasing the applied potential results in little change to the deposit composition. This study indicates that the concentration of $CdSO_4$ is critical to maintain a proper composition of the deposit.

Effect of pH.—pH of the electrolyte determines the concentration of the electroactive species present at the interface and thereby controls the deposition potential. Figure 4 shows the effect of pH on the deposition of Zn-Ni-Cd ternary alloy as a function of deposition potential. When the pH of the electrolytic bath is increased, the Zn and Ni deposition potentials, in particular, appear to shift to more negative values. The nickel composition in the codeposit decreases and the cadmium composition increases with increasing pH. The composition values given in Fig. 4 have been normalized based on Zn, Ni, and Cd composition values, and the real changes in the compositions of nickel and cadmium are not clearly seen. Figure 5 shows the partial current density of Ni and Cd deposited at different pH conditions. It is seen that increasing the pH has more influence on the Ni content compared to the other elements. The Ni partial current density measured at -1.4 V *vs.* SCE decreases to 66.5% with increasing the pH of the electrolyte. Cadmium partial current reaches a limiting current density at around -1.2 V *vs.* SCE, and its value decreases by 6.7% with increasing the pH from 9.3 to 11.3.

Figure 6 shows the calculated equilibrium concentrations of the electroactive species in the Zn-Ni-Cd plating bath as a function of pH. The concentrations of all electroactive species in the bath were determined by using various element balances, equilibrium conditions, and the electroneutrality conditions at a specified pH. The governing equations and the computational details are summarized and shown in the Appendix. As the pH increases, the concentration of bivalent ions decreases, and all species under neutral to mildly acidic conditions exist as monohydroxides. In alkaline conditions the electroactive species do not exist in its ionic form, and the concentration of the monohydroxides are negligible. In the absence of a stabilizing agent, all electroactive species precipitate in alkaline conditions. In the presence of ammonia, the following complex ions are formed

$$Zn^{2+} + 2\ OH^- \rightarrow Zn(OH)_2$$

$$Zn(OH)_2 + 4NH_3 \rightarrow Zn(NH_3)_4^{2+} + 2\ OH^-$$

$$Ni^{2+} + 2\ OH^- \rightarrow Ni(OH)_2$$

$$Ni(OH)_2 + 6NH_3 \rightarrow Ni(NH_3)_6^{2+} + 2\ OH^-$$

$$Cd^{2+} + 2\ OH^- \rightarrow Cd(OH)_2$$

$$Cd(OH)_2 + 4NH_3 \rightarrow Cd(NH_3)_4^{2+} + 2\ OH^-$$

The ammonia is released through the following redox reactions

$$Zn(NH_3)_4^{2+} + 2e \rightarrow Zn + 4NH_3$$

$$Ni(NH_3)_6^{2+} + 2e \rightarrow Ni + 6NH_3$$

$$Cd(NH_3)_4^{2+} + 2e \rightarrow Cd + 4NH_3$$

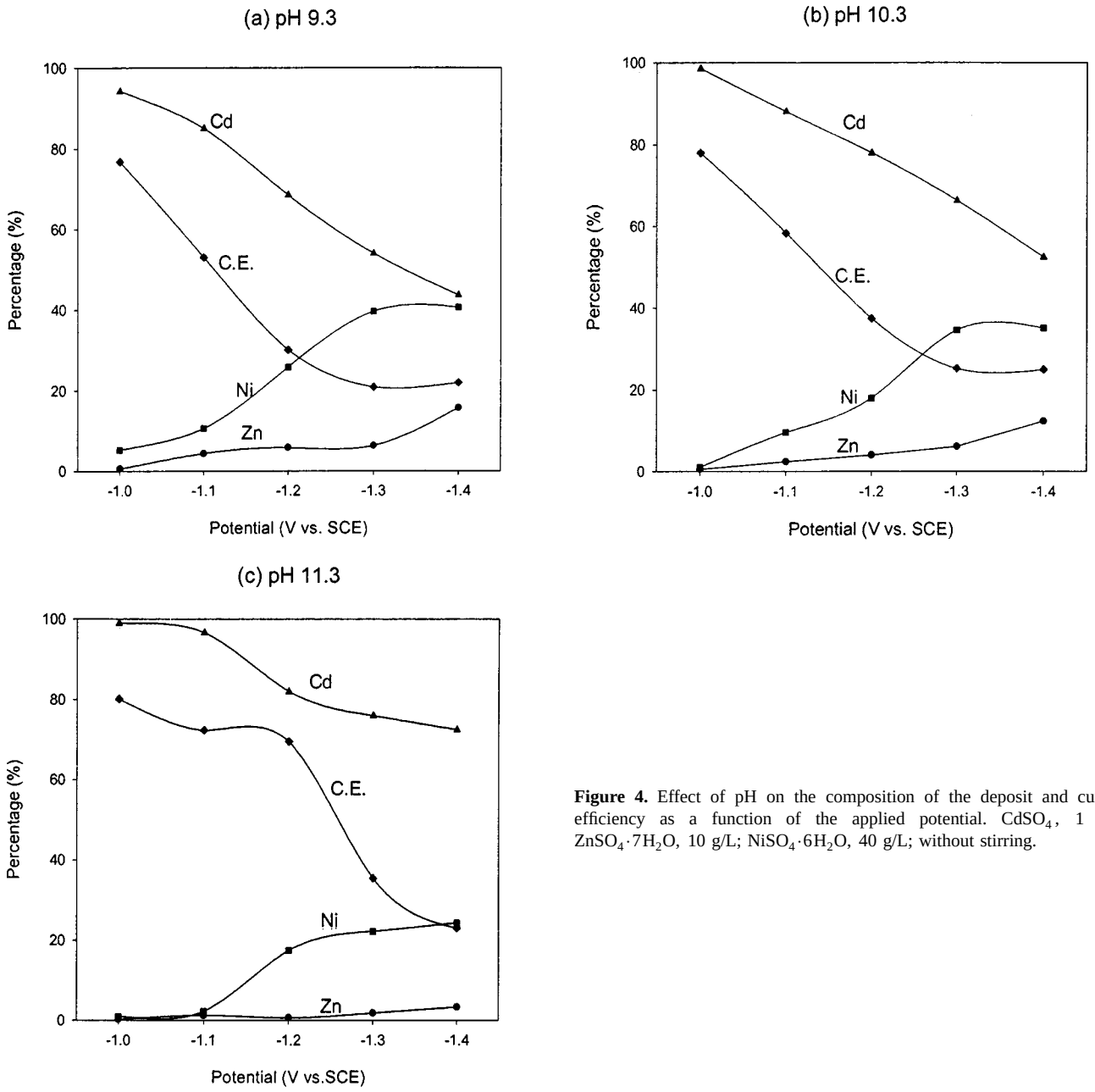

Figure 4. Effect of pH on the composition of the deposit and current efficiency as a function of the applied potential. $CdSO_4$, 1 g/L; $ZnSO_4 \cdot 7H_2O$, 10 g/L; $NiSO_4 \cdot 6H_2O$, 40 g/L; without stirring.

As shown in Fig. 6, the nickel complex ion is stable up to pH 9.8. However, at pH higher than 9.8, the concentration of this complex starts to decrease drastically. The $[Cd(NH_3)_4^{2+}]$ concentration in the electrolyte shows a very small change as a function of pH when compared to the Ni complex ion concentration. Since the Ni content in the deposit significantly decreases with increasing the pH, the normalized Cd content in the deposit increases. Thus, the results indicate that the Ni content in the deposit strongly depends on pH. One can expect that electrodeposition from electrolytes with pH lower that 9.8 will result in deposits with high Ni and low Cd content.

Effect of stirring.—All deposition processes discussed above were carried out without stirring. Zn and Cd depositions are mass-transfer limited processes, and therefore, stirring has a significant effect on their deposition kinetics. Figure 7 shows the composition analysis for each component with varying the stirring speed. The depositions were performed at −1.3 V from a solution containing 1 g/L of $CdSO_4$, 10 g/L of $ZnSO_4 \cdot 7H_2O$, and 40 g/L of $NiSO_4 \cdot 6H_2O$ at a pH of 9.3. Increasing the stirring speed increases the content of Cd in the deposit while reducing the Ni content. The results can be explained by taking into account the fact that Cd is mass-transfer controlled. The observed decrease in the Ni content results from a mass-transfer control of the competing proton, Zn and Cd reduction processes. Increasing the stirring speed causes more of these ions to be present near the electrode surface, which increases their deposition rate.

Effect of $ZnSO_4 \cdot 7H_2O$ concentration and additives.—Zinc composition in the deposit can be improved by either decreasing the cadmium concentration (thus decreasing the limiting current density of Cd deposition) or by increasing the $ZnSO_4 \cdot 7H_2O$ concentration. Figure 8 shows the effect of $ZnSO_4 \cdot 7H_2O$ concentration on the deposit compositions. The concentration of $NiSO_4 \cdot 6H_2O$ was fixed to be 40 g/L. The deposition was carried out potentiostatically at −1.3 V *vs.* SCE at pH 9.3 without stirring. In the case of 1 g/L of $CdSO_4$, increasing the $ZnSO_4 \cdot 7H_2O$ in the electrolyte results in a

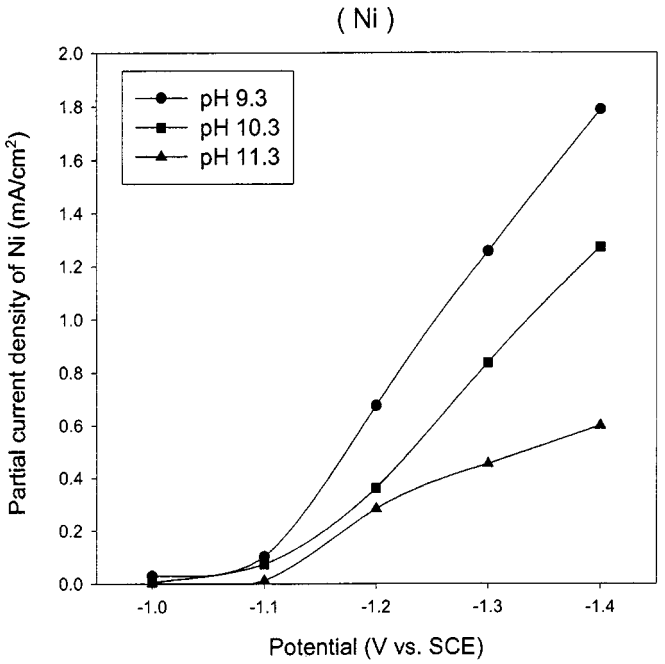

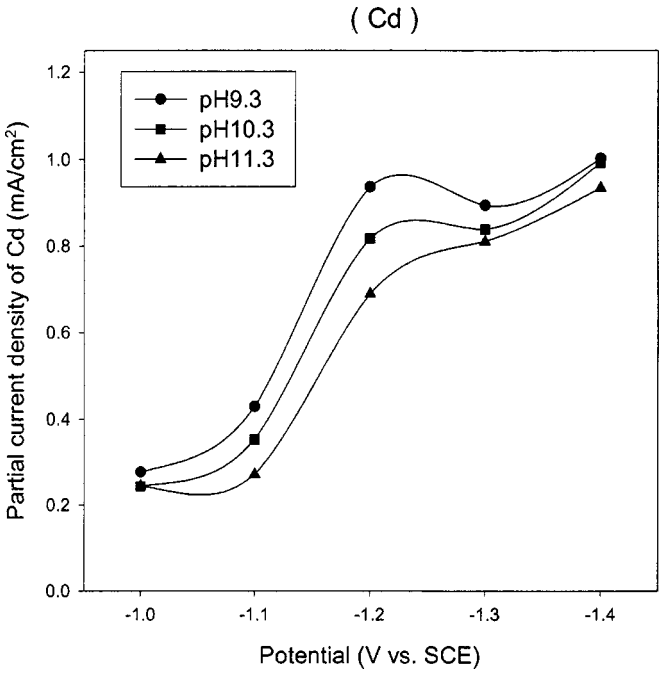

Figure 5. Effect of pH on the partial current density of Ni and Cd as a function of the applied potential.

decrease of Cd content in the deposit up to 17% with a small change in the Ni content. However, when the $CdSO_4$ concentration in the bath is higher than 1 g/L, an increase in the concentration of $ZnSO_4 \cdot 7H_2O$ does not result in any significant effects on the deposit composition. The results indicated that the $CdSO_4$ concentration in the electrolyte controls the deposit composition. The $CdSO_4$ concentration in the electrolyte should be maintained below 1 g/L in order to obtain deposits with high Zn and Ni contents.

Figure 9 shows the effect of $ZnSO_4 \cdot 7H_2O$ concentration on the deposition current density as a function of deposition time. The electrolysis time was kept a constant at 1 h. The deposition current density follows a unique pattern in which the current density is stable for some portion of the experiment and increases steeply after

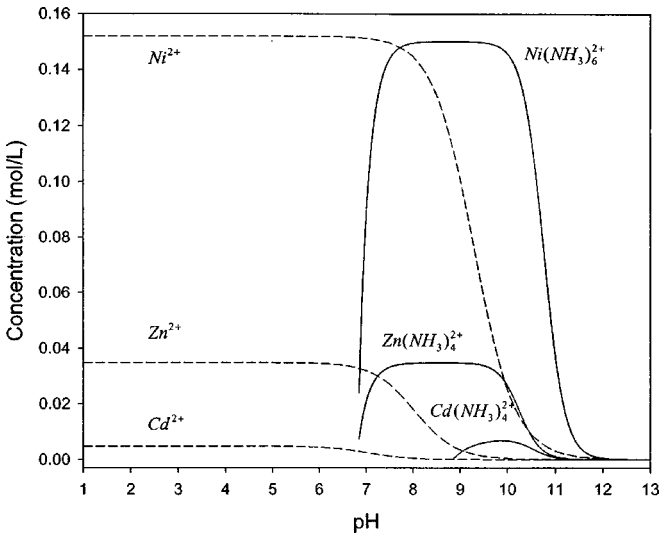

Figure 6. Solution equilibrium concentration in Zn-Ni-Cd plating bath as a function of pH.

that. With increasing the concentration of $ZnSO_4 \cdot 7H_2O$ in the bath, the stable portion plateau increases. Such changes in current density modify the morphology and composition of the deposits. SEM and EDX analyses were carried out to study the changes in morphology and composition of the deposits due to the changes in current density. Figure 10 shows the surface morphology of the deposits taken at three points indicated in Fig. 9; one on the stable plateau, one when the sudden change in current density happens, and one at the end of the experiment when the second change in current density occurs. The SEM image showed uniform grain particle deposited at the first plateau area, and it has a composition ratio of 47/28/25 for Zn/Ni/Cd, respectively. When the current density starts to increase at point 2, dendrite growth was detected on the top of the grain deposition. EDX analysis of the dendrite cluster showed a composition ratio of 4/19/77 (Zn/Ni/Cd) which has a higher Cd content compared to the background deposition. After reaching steady-current density

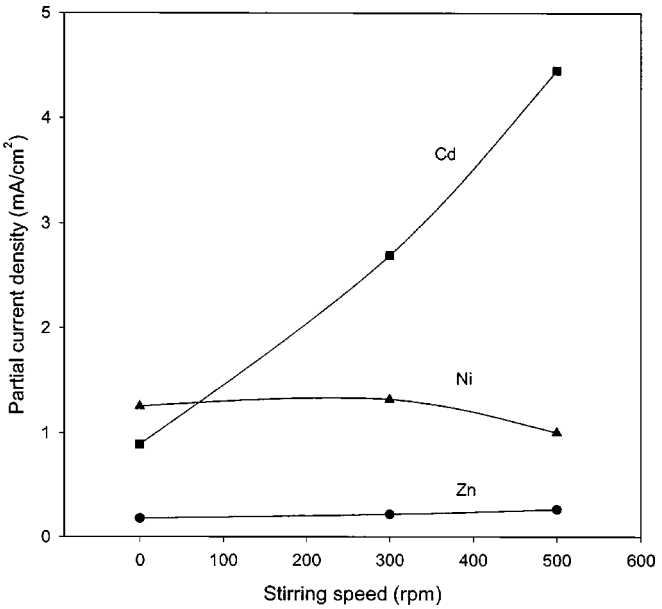

Figure 7. Dependence of the stirring speed on the alloy composition of Zn, Ni, and Cd obtained from the solution of $CdSO_4$, 1 g/L; $ZnSO_4 \cdot 7H_2O$, 10 g/L; $NiSO_4 \cdot 6H_2O$, 40 g/L at pH 9.3.

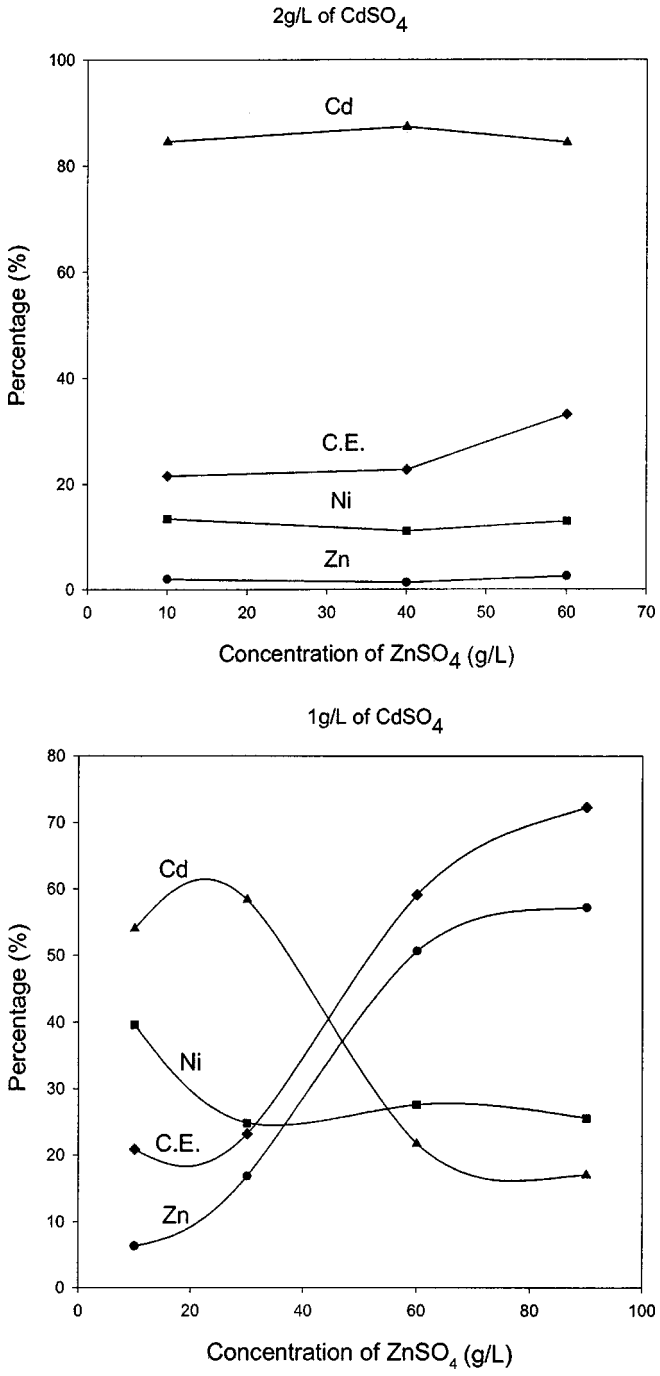

Figure 8. Effect of $ZnSO_4 \cdot 7H_2O$ concentration on the alloy composition and current efficiency when the concentration of $CdSO_4$ are 1 g/L and 2 g/L. $NiSO_4 \cdot 6H_2O$, 40 g/L; pH 9.3; V, −1.3 V *vs.* SCE, no stirring.

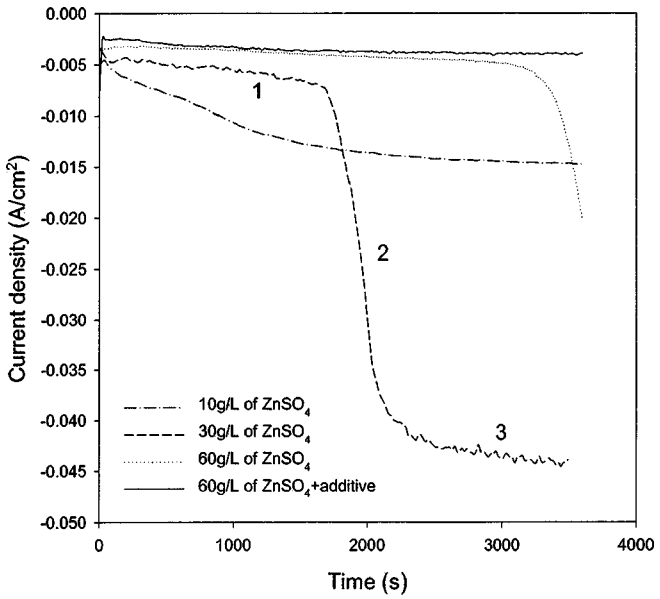

Figure 9. Effect of $ZnSO_4 \cdot 7H_2O$ concentration and additive on the deposition current density as a function of time.

again, the SEM showed the increase in size of the dendrite clusters. Because a dendrite cluster has a higher Cd content, the average composition ratio was changed to 17/25/58 (Zn/Ni/Cd), which indicates that deposition of Cd proceeded strongly with time during dendrite formation. Besides increasing the Cd content enormously, the dendrites have poor adhesion and are easily removed from the surface with washing. This imposes a limit on the thickness of the adherent film. Increasing the concentration of $ZnSO_4 \cdot 7H_2O$ extends the duration of the first current density plateau, thereby giving rise to thicker layers of uniform deposit. However, increasing the concentration of $ZnSO_4 \cdot 7H_2O$ also alters the deposit composition and thereby the deposit properties. Next organic additives were used to improve the deposit adherence on the substrate and to prevent the dendrite formation. Out of several additives tested, when 0.4 g/L of dextrin and 30 g/L of sodium citrate were added to the deposit bath, a constant current density was observed over the entire deposition time. The deposits obtained were homogeneous and have good adhesion. Figure 11 shows a SEM image of the deposit prepared in the presence of the additive. The deposits are dense with a well-organized structure compared to the deposits prepared in the absence of additives in the electrolyte. The EDX analysis showed a composition of 50/28/22 for Zn/Ni/Cd. The additives also increase the overpotential of hydrogen evolution reaction, resulting in an increase of the current efficiency from 59 to 96%.

Conclusions

Electrodeposition of the Zn-Ni-Cd from complex ion bath was studied as a function of pH, concentrations of the electroactive species in the electrolyte, and stirring. Cd deposition was found to be mass-transfer controlled and dominates the entire alloy deposition process. The concentrations of all electroactive species in the bath were determined by using material balances of the elements, equilibrium conditions, and the electroneutrality conditions at a specified pH. Under neutral to mildly alkaline conditions, the concentration of bivalent cations decreases and all species exist as monohydroxides. In alkaline conditions none of the species exists in its ionic form and the concentration of the monohydroxides are negligible. Nickel and zinc precipitate in alkaline conditions without stabilizing agents. In this study, to maintain the stability of the bath sodium citrate and ammonium hydroxide were used as complexing agents. The Ni content in the deposit significantly decreases with increasing the pH, while the Cd content in the deposit increases. The deposits plated at a pH lower than 9.8 exhibit high Ni and low Cd content. Increasing the stirring speed increases the content of Cd in deposit while reducing the Ni content. The observed decrease in the Ni content resulted from a mass-transfer control of the competing proton, Zn and Cd reduction processes. At concentrations of $CdSO_4$ higher than 1 g/L in the bath, the limiting current density of cadmium increases leading to a deposition of large amounts of Cd in the deposit. Increasing the $ZnSO_4 \cdot 7H_2O$ concentration in the bath led to an increase in the Zn content in the deposit by mainly replacing the Cd content.

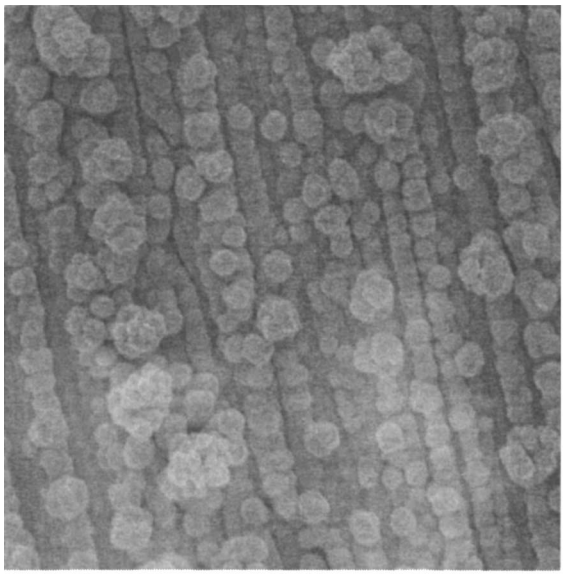

(1) 47/28/25 (Zn/Ni/Cd)

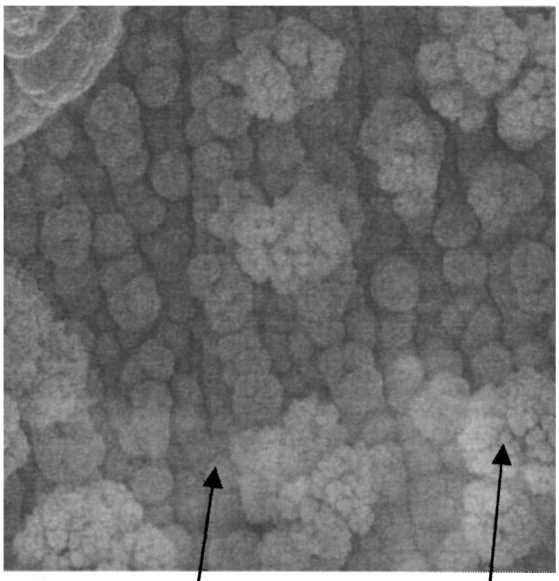

(2) 47/28/25 (Zn/Ni/Cd)

4/19/77 (Zn/Ni/Cd)

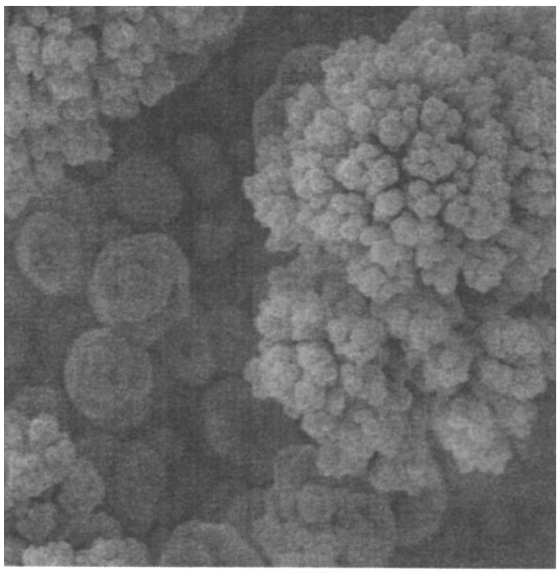

(3) 17/25/58 (Zn/Ni/Cd)

Figure 10. Surface morphology and composition analysis corresponding to three distinct points depicted in Fig. 9.

Acknowledgments

Financial Support by Dr. Vinod Agarvala, the Office of Naval Research under grant no. N00014-00-1-0053 and AESF Research Contract, Project 107, are gratefully acknowledged. This work was also partially supported by Sandia National Laboratories. Sandia is a multiprogram laboratory operated by Sandia Corporation, a Lockheed Martin Company, for the United States Department of Energy under contract DE-AC04-94-AL85000.

The University of South Carolina assisted in meeting the publication costs of this article.

Appendix

The electrodeposition bath consists of 1 g/L of $CdSO_4$, 10 g/L of $ZnSO_4 \cdot 7H_2O$, 40 g/L of $NiSO_4 \cdot 6H_2O$, and 0.9 M of NH_3. The variables to be determined are as follows: $[Zn^{2+}]$, $[Ni^{2+}]$, $[Cd^{2+}]$, $[Zn(OH)^{+}]$, $[Ni(OH)^{+}]$, $[Cd(OH)^{+}]$, $[Zn(OH)_2]$, $[Ni(OH)_2]$, $[Cd(OH)_2]$, $[Zn(NH_3)_4^{2+}]$, $[Ni(NH_3)_6^{2+}]$, $[Cd(NH_3)_4^{2+}]$, $[Zn_2(OH)^{3+}]$, $[OH^{-}]$, $[SO_4^{2-}]$, and $[HSO_4^{-}]$. The concentration of $[H^{+}]$ depends on the specified pH. The equations used to determine the concentrations are

1. Material balance on zinc

$$[ZnSO_4]_{ad} = [Zn^{2+}] + [Zn(OH)^{+}] + 2[Zn_2(OH)^{3+}] + [Zn(OH)_2] + [Zn(NH_3)_4^{2+}]$$

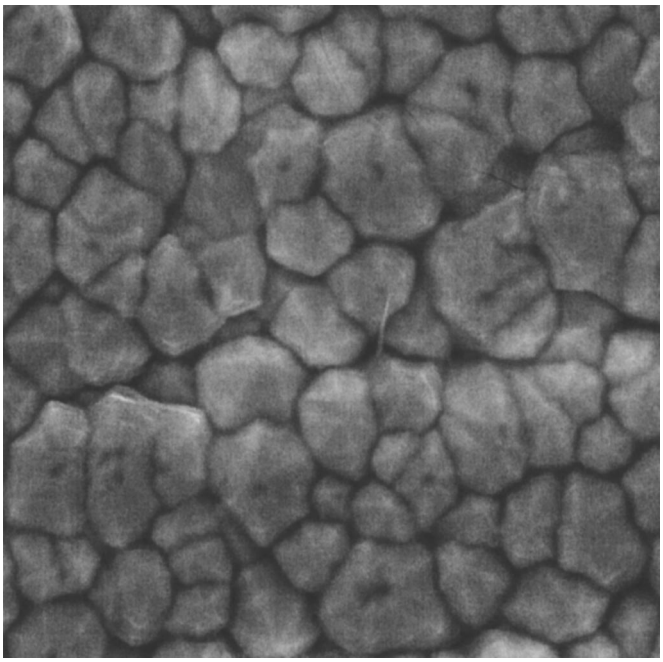

Figure 11. SEM image of Zn-Ni-Cd deposit obtained from the bath containing additives, 0.4 g/L of dextrin and 30 g/L of sodium citrate

2. Material balance on nickel

$$[NiSO_4]_{ad} = [Ni^{2+}] + [Ni(OH)^+] + [Ni(OH)_2] + [Ni(NH_3)_6^{2+}]$$

3. Material balance on cadmium

$$[CdSO_4]_{ad} = [Cd^{2+}] + [Cd(OH)^+] + [Cd(OH)_2] + [Cd(NH_3)_4^{2+}]$$

4. The electroneutrality

$$[H^+] + 2[Zn^{2+}] + 2[Ni^{2+}] + 2[Cd^{2+}] + [Zn(OH)^+] + [Ni(OH)^+] + [Cd(OH)^+] + 3[Zn_2(OH)^{3+}] + 2[Zn(NH_3)_4^{2+}] + 2[Ni(NH_3)_6^{2+}] + 2[Cd(NH_3)_4^{2+}] = [HSO_4^-] + 2[SO_4^{2-}] + [OH^-]$$

5. The equilibrium conditions

$$[H^+][SO_4^{2-}] - k1[HSO_4^-] = 0$$

$$[Zn^{2+}][OH^-] - k2[Zn(OH)^+] = 0$$

$$[Ni^{2+}][OH^-] - k3[Ni(OH)^+] = 0$$

$$[Cd^{2+}][OH^-] - k4[Cd(OH)^+] = 0$$

$$[H^+][OH^-] - k5 = 0$$

$$[Zn^{2+}][OH^-]^3 - k6[Zn_2(OH)^{3+}] = 0$$

$$[Zn(OH)^+][OH^-] - k7 = 0$$

$$[Ni(OH)_2][OH^-] - k8 = 0$$

$$[Cd(OH)_2][OH^-] - k9 = 0$$

$$[Zn(OH)_2][NH_3]_{ad}^4 - k10[Zn(NH_3)_4^{2+}][OH^-]^2 = 0$$

$$[Ni(OH)_2][NH_3]_{ad}^6 - k11[Ni(NH_3)_6^{2+}][OH^-]^2 = 0$$

$$[Cd(OH)_2][NH_3]_{ad}^4 - k12[Cd(NH_3)_4^{2+}][OH^-]^2 = 0$$

These equations were solved simultaneously by using MAPLE.

References

1. S. Swathirajan, *J. Electrochem. Soc.*, **133**, 671 (1986).
2. G. W. Loar, K. R. Romer, and T. J. Aoe, *Plat. Surf. Finish.*, **78**, 74 (1991).
3. M. F. Mathias and T. W. Chapman, *J. Electrochem. Soc.*, **134**, 1408 (1987).
4. M. S. Michael, M. Pushpavanam, and K. Balakrishnan, *Br. Corros. J., London*, **30**, 317 (1995).
5. I. Kirilova, I. Ivanov, and St. Rashkov, *J. Appl. Electrochem.*, **27**, 1380 (1997).
6. A. Brenner, *Electrodeposition of Alloys*, Vol. II, Academic Press, New York (1963).
7. N. S. Grigoryan, V. N. Kudryavtsev, P. A. Zhdan, I. Y. Kolotyrkin, E. A. Volynskaya, and T. A. Vagramyan, *Zasch. Met.*, **25**, 288 (1989).
8. E. Hall, *Plat. Sur. Finish.*, **70**, 59 (1983).
9. M. Pushpavanam, S. R. Natarajan, K. Balakrishana, and L. R. Sharma, *J. Appl. Electrochem.*, **21**, 642 (1991).
10. K. Higaashi, H. Fukushima, T. Urakawa, T. Adaniya, and K. Matsudo, *J. Electrochem. Soc.*, **128**, 2081 (1981).
11. F. Elkhatabi, M. Benballa, M. Sarret, and C. Muller, *Electrochim. Acta*, **44**, 1645 (1999).
12. A. Krishniyer, M. Ramasubramanian, B. N. Popov, and R. E. White, *Plat. Surf. Finish.* **1**, 99 (1999).
13. S. Swathirajan and Y. M. Mikhail, *J. Electrochem. Soc.*, **136**, 2189 (1989).
14. A. Durairajan, A. Krishniyer, B. N. Popov, B. Haran, and R. E. White, *Corrosion (Houston)*, **56**, 283 (2000).
15. Z. Zhou and T. J. O. Keefe, *Surf. Coat. Technol.*, **96**, 191 (1997).
16. A. Durairajan, B. Haran, R. E. White, and B. N. Popov, *J. Electrochem. Soc.*, **147**, 48 (2000).
17. A. Durairajan, B. Haran, R. E. White, and B. N. Popov, *J. Electrochem. Soc.*, **147**, 4507 (2000).
18. A. Durairajan, Ph.D. Thesis, University of South Carolina, Columbia, SC (2001).
19. B. N. Popov, M. Ramasubramanian, S. N. Popova, R. E. White, and K.-M. Yin, *J. Chem. Soc., Faraday Trans.*, **92**, 4021 (1996).
20. B. N. Popov, S. N. Popova, K.-M. Yin, and R. E. White, *Plat. Surf. Finish.*, **1994**, 65 (March).